Supporting Information

On the role played by the chalcogen donor atoms in diimine-dichalcogenolate Pt^{II} SONLO chromophores: is it worth replacing sulfur with selenium?

Anna Pintus, M. Carla Aragoni, Francesco Isaia, Vito Lippolis, Dominique Lorcy,

Alexandra M. Z. Slawin, J. DerekWoollins, and Massimiliano Arca*

Experimental part

Chemicals: 2,2'-Bipyridine, 1,10-phenanthroline, K_2PtCl_4, ethyl alcohol, and thf were obtained from commercial sources and purified when necessary by using standard techniques.

Synthesis of Complexes: Platinum dichlorodiimine complexes [Pt(bipy)Cl_2], [Pt(phen)Cl_2],[1,2] and *N*-methyl-4,5-*bis*(2'-cyanoethylseleno)-1,3-thiazol-2-thione [3] were synthesized according to published procedures. The complexes [Pt(bipy)(Me-dmet)] (**4**) and [Pt(phen)(Me-dmet)] (**5**) were synthesized and characterized as described in a previous work.[4]

[Pt(bipy)(Me-dset)] (1). A dry ethyl alcohol solution of sodium ethoxyde (15 mL; 3.6 mmol) was added dropwise to a solution of *N*-substituted-4,5-*bis*(2'-cyanoethylseleno)-1,3-thiazol-2-thione in the same solvent (15 mL; 0.18 g, 0.45 mmol) under a N_2 atmosphere. A suspension of [Pt(bipy)Cl_2] (0.19 g, 0.45 mmol) in 20 mL of dry thf was then added dropwise, and the reaction mixture was left under magnetic stirring for one week, after which the solvent was removed under reduced pressure. The crude product obtained was then suspended in 600 mL of CH_2Cl_2, and 100 mL of *n*-hexane were added dropwise to the filtered solution, resulting in the precipitation of a dark solid, which was collected by filtration. X-ray quality crystals were obtained by slow infusion of petroleum ether into a CH_2Cl_2 solution of the complex. Yield: 0.02 g (9 %); m.p. > 240° C; FT-IR: $\tilde{\nu}$ = 411 (w), 481 (w), 517 (s), 638 (w), 712 (s), 747 (vs), 761 (m), 789 (w), 906 (w), 925 (w), 990 (m), 1068 (m), 1124 (vs), 1158 (w), 1246 (w), 1316 (m), 1336 (m), 1384 (w), 1432 (w), 1446 (s), 1471 (s), 1498 (m), 1604 (m), 3068 cm^{-1} (vw); UV-Vis-NIR (dmso): λ (ε) = 257 (17000), 277 (16000), 302 (16000), 331 (6000), 371 (11000), 569 nm (3500 M^{-1} cm^{-1}); fluorescence (dmso; λ_{exc} = 341 nm; slit = 5x5): λ_{em} = 374, 394 nm, Φ = $8.21 \cdot 10^{-3}$; ^{1}H-NMR (dmso-d_6): δ = 9.00 (d, 1H), 8.90 (d, 1H), 8.79 (d, 2H), 8.54 (t, 2H), 8.00 (t, 2H), 3.74 (s, 3H) ppm; elemental analysis calcd (%) for $C_{14}H_{11}N_3S_2Se_2Pt$: C 26.34, H 1.74, N 6.58, S 10.05; found: C 25.76, H 1.63, N 6.02, S 9.04; CV (dmso): $E_{1/2}$ *vs* Fc^+/Fc (scan rate = 50 mV s^{-1}) = –2.245, –1.607, 0.044 V.

[Pt(phen)(Me-dset)] (2). The complex was synthesized as described for [Pt(bipy)(Me-dset)] (**1**) starting from [Pt(phen)Cl_2] (0.14 g, 0.31 mmol). Yield: 0.11 g (55 %); m.p. > 240° C; FT-IR: $\tilde{\nu}$ =

502 (w), 517 (s), 650 (w), 705 (vs), 724 (m), 754 (w), 787 (w), 831 (s), 916 (m), 990 (s), 1063 (m), 1126 (s), 1151 (w), 1217 (w), 1294 (w), 1340 (m), 1430 (m), 1502 (m), 1578 cm^{-1} (w); UV-Vis-NIR (dmso): λ (ε) = 271 (41000), 374 (16000), 570 nm (5000 M^{-1} cm^{-1}); Fluorescence (dmso; λ_{ecx} = 279 nm; slit = 5x5): λ_{em} = 373, 392 nm, $\Phi = 1.18 \cdot 10^{-2}$; ^{1}H NMR (dmso-$d_6$): 9.36 (d, 1H), 9.26 (d, 1H), 9.16 (d, 2H), 8.40 (d, 2H), 8.22 (t, 2H), 3.78 (s, 3H) ppm; elemental analysis calcd (%) for $C_{16}H_{11}N_3S_2Se_2Pt$: C 29.01, H 1.67, N 6.34, S 9.68; found: C 30.93, H 2.38, N 7.21, S 8.40; CV (dmso): $E_{1/2}$ *vs* Fc^+/Fc (scan rate = 100 mV s^{-1}) = –1.620, –0.027 V.

Characterization: Elemental analyses were performed with an EA1108 CHNS-O Fisons Instrument (T = 1000° C). FT-IR spectra were recorded with a Thermo-Nicolet 5700 spectrometer at room temperature: KBr pellets with a KBr beam-splitter and KBr windows (4000–400 cm^{-1}, resolution 4 cm^{-1}) were used. ^{1}H-NMR spectra were recorded on a Varian INOVA 400 MHz spectrometer at 298 K and referenced to $Si(CH_3)_4$. Absorption spectra were recorded at 298 K in a quartz cell of 10.00 mm optical path with a Thermo Evolution 300 (190–1100 nm) spectrophotometer. Uncorrected emission spectra were collected at 298 K with a Varian Cary Eclipse spectrophotometer equipped with a xenon lamp. Quantum yields were determined relative to anthracene in ethyl alcohol ($C = 1–5 \cdot 10^{-6}$ M; λ_{exc} = 334–359 nm), by calculating the integrated emission intensity of both the sample and the reference through a decomposition of the spectra in their constituent Gaussian curves. Spectral decomposition was carried out by means of the software Fytik.[5] Cyclic voltammetry measurements (scan rate 10–1000 mV s^{-1}) were performed in anhydrous dmso in a Metrohm voltammetric cell, with a combined working and counter platinum electrode and a standard Ag/AgCl reference electrode with a Metrohm Autolab PGSTAT 10 potentiostat (supporting electrolyte (TBA^+)(PF_6^-) 0.10 M): reported data are referred to the Fc^+/Fc reversible couple.

X-ray crystallography: Single crystal X-ray diffraction data for complex **1** were collected with the St. Andrews Robotic diffractometer at 125(2) K.

Insert Ref A. L Fuller, L. A. S. Scott-Hayward, Y. Li, M. Bühl , A. M. Z. Slawin and J. D. Woollins, *J. Am. Chem. Soc.*, 2010**, 132** , 5799–5802. **DOI:** 10.1021/ja100247y

The structures were solved by direct methods with SHELXS-97[6] and refined on F^2 by using SHELXL2013.[7] I doin't know how to use Endnote.,..the correct Ref for SHELX is now Sheldrick, G. M. (2008). Acta Cryst. A64, 112–122.

DFT Calculations: Theoretical calculations were performed at DFT level [8] with the Gaussian 09 suite of programs (Rev. A.02)[9] on a E4 workstation equipped with four quad-core AMD Opteron processors and 16 Gb of RAM and running the 64 bit version of the Ubuntu 12.04 Linux operating system. The PBE0 (PBE1PBE) hybrid functional was adopted,[10] and Schäfer, Horn, and Ahlrichs double-ζ plus polarization all-electron basis sets[11] were used for C, H, N, S and Se, whereas CRENBL BS[12] with relativistic effective core potentials (RECPs)[13,14] was chosen for the heavier Pt species. Preliminary calculations were performed on complex **1** by employing the CRENBL-ECP BSs also on the Se atoms, in order to account for the relativistic effects for this atomic species, but no significant improvement was observed to be conferred to the agreement between experimental and calculated data upon employing ECPs,[15] and thus the Ahlrichs BS was eventually employed on all atomic species but the metal. The geometry of the complexes was optimized starting from structural data when available, and tight SCF convergence criterion (*SCF=tight* keyword) and fine numerical integration grids [*Integral(FineGrid)* keyword] were used. The nature of the minima of each optimised structure was verified by harmonic frequency calculations (*freq=raman* keyword). NBO charges distributions[16] and Wiberg[17] bond indices were calculated at the optimized geometries. Electronic transition energies and oscillator strength values were calculated at TD-DFT level (100 states). The electronic spectra were simulated by a convolution of Gaussian functions centered at the calculated excitation energies. In order to determine the influence of the solvent on the properties of the

complexes, solvation calculations were also carried out in dmso, implicitly taken into account by means of the polarizable continuum model (PCM) in its integral equation formalism variant (IEF-PCM).[18] The total static second-order (quadratic) hyperpolarizability (the first hyperpolarizability)[19] β_{tot} was calculated as described previously.[4,20] The programs Gaussview 5.0,[21] and Molden 5.0[22] were used to investigate the charge distributions and molecular orbital shapes. The software GaussSum 2.1[23] was used to calculate the molecular orbital contributions (MOC) from groups of atoms, along with the contribution of singly excited configurations to each electronic transition, and to generate all the necessary data to simulate absorption spectra.

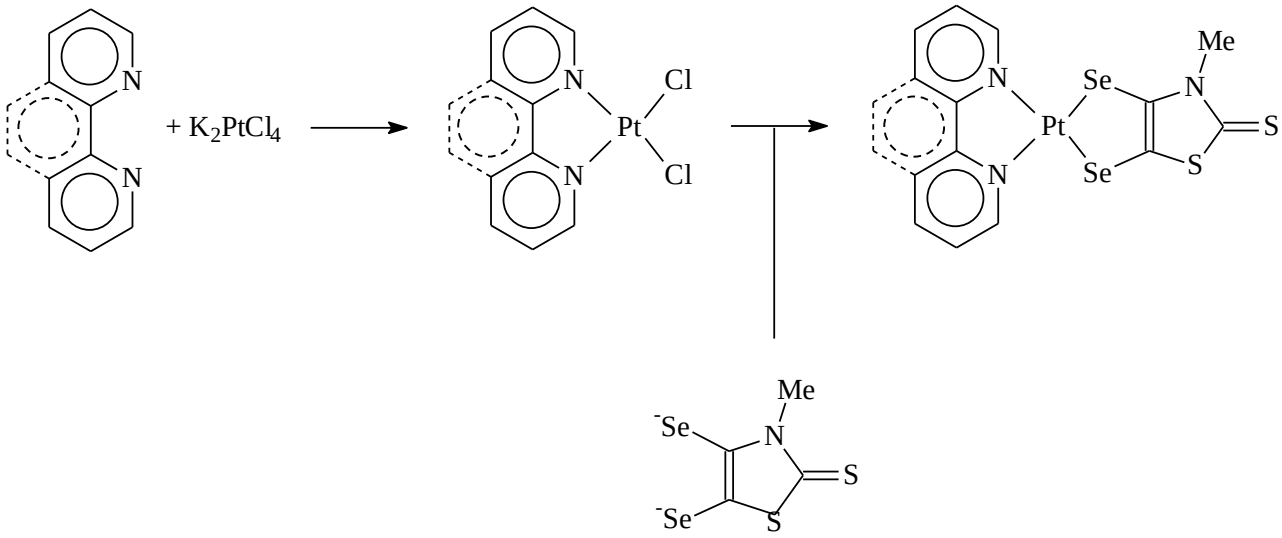

Scheme S1. General pathway for the synthesis of [Pt(N^N)(Me-dset)] complexes **1** and **2**.

Table S1. Crystal data and details of the structure determination for compound **1**·1/2CH_2Cl_2.

Formula		C14.5 H12 Cl N3 Pt S2 Se2	
Formula Weight			680.86
Crystal System			Triclinic
Space group		P-1	(No. 2)
a, b, c [Å]	8.0202(13)	8.2543(14)	14.153(3)
α, β, γ[°]	105.827(13)	97.865(18)	99.619(17)
V [Å^3]			872.2(3)
Z			2
D(calc) [g/cm^3]			2.592
Mu(MoKa) [/mm]			12.579
F(000)			630
Crystal Size [mm]		0.03 x 0.03 x 0.15	
Temperature (K)			125
Radiation [Å]		MoKa	0.71075
Theta Min-Max [°]			2.6, 26.4
Dataset		-9: 9 ; -10: 10 ; -17: 17	
Tot., Uniq. Data, R(int)		7208, 3441, 0.052	
Observed data [I > 0.0 sigma(I)]			3175
Nref, Npar			3441, 218
R, wR2, S		0.0533, 0.1354, 1.06	
Max. and Av. Shift/Error			0.00, 0.00
Min. and Max. Resd. Dens. [e/ Å ^{3}]			-2.86, 2.00

Table S2. Bond distances (Å) for compound **1**·1/2CH_2Cl_2.

Pt1	-Se21	2.3929(12)	C5	-C6	1.382(15)
Pt1	-Se22	2.3803(13)	C6	-C8	1.484(16)
Pt1	-N1	2.078(9)	C8	-C9	1.391(16)
Pt1	-N7	2.060(9)	C9	-C10	1.407(15)
Se21	-C23	1.883(11)	C10	-C11	1.393(16)
Se22	-C27	1.881(11)	C11	-C12	1.370(15)
Cl31	-C30	1.94(3)	C23	-C27	1.331(15)
Cl31	-C30_a	1.58(3)	C2	-H2	0.9500
S24	-C25	1.744(11)	C3	-H3	0.9500
S24	-C23	1.740(10)	C4	-H4	0.9500
S27	-C25	1.662(12)	C5	-H5	0.9500
N1	-C6	1.381(14)	C9	-H9	0.9500
N1	-C2	1.323(14)	C10	-H10	0.9500
N7	-C8	1.357(14)	C11	-H11	0.9500
N7	-C12	1.315(14)	C12	-H12	0.9500
N26	-C27	1.417(14)	C28	-H28C	0.9800
N26	-C25	1.369(14)	C28	-H28A	0.9800
N26	-C28	1.447(14)	C28	-H28B	0.9800
C2	-C3	1.378(16)	C30	-H30A	0.9900
C3	-C4	1.363(16)	C30	-H30B	0.9900
C4	-C5	1.379(16)			

See Table S5 for translation of symmetry code to equivalent positions.

Table S3. Angles (°) for compound **1**·1/2CH_2Cl_2.

Se21	-Pt1	-Se22	91.26(4)	N7	-C8	-C6	116.1(10)
Se21	-Pt1	-N1	174.6(3)	C8	-C9	-C10	119.0(10)
Se21	-Pt1	-N7	95.0(2)	C9	-C10	-C11	117.9(10)
Se22	-Pt1	-N1	93.3(3)	C10	-C11	-C12	118.7(10)
Se22	-Pt1	-N7	173.8(2)	N7	-C12	-C11	124.4(10)
N1	-Pt1	-N7	80.5(4)	Se21	-C23	-C27	123.0(8)
Pt1	-Se21	-C23	100.2(3)	S24	-C23	-C27	110.1(8)
Pt1	-Se22	-C27	100.1(3)	Se21	-C23	-S24	126.9(6)
C30	-Cl31	-C30_a	68.2(14)	S24	-C25	-N26	108.4(8)
C23	-S24	-C25	93.0(5)	S27	-C25	-N26	127.7(8)
Pt1	-N1	-C2	127.0(8)	S24	-C25	-S27	123.9(7)
C2	-N1	-C6	119.7(9)	Se22	-C27	-C23	124.1(8)
Pt1	-N1	-C6	113.2(7)	N26	-C27	-C23	114.2(9)
Pt1	-N7	-C8	114.4(7)	Se22	-C27	-N26	121.6(7)
Pt1	-N7	-C12	127.1(7)	C3	-C2	-H2	119.00
C8	-N7	-C12	118.4(10)	N1	-C2	-H2	119.00
C25	-N26	-C27	114.3(8)	C2	-C3	-H3	121.00
C25	-N26	-C28	122.2(9)	C4	-C3	-H3	121.00
C27	-N26	-C28	123.5(9)	C5	-C4	-H4	120.00
N1	-C2	-C3	122.2(11)	C3	-C4	-H4	120.00
C2	-C3	-C4	118.7(11)	C4	-C5	-H5	120.00
C3	-C4	-C5	120.5(10)	C6	-C5	-H5	120.00
C4	-C5	-C6	119.0(11)	C10	-C9	-H9	120.00
N1	-C6	-C8	115.4(9)	C8	-C9	-H9	121.00
C5	-C6	-C8	124.8(10)	C9	-C10	-H10	121.00
N1	-C6	-C5	119.8(10)	C11	-C10	-H10	121.00
N7	-C8	-C9	121.6(10)	C12	-C11	-H11	121.00
C6	-C8	-C9	122.4(10)	C10	-C11	-H11	121.00
N7	-C12	-H12	118.00	H28A	-C28	-H28B	109.00
C11	-C12	-H12	118.00	Cl31	-C30	-Cl31_a	111.8(16)
N26	-C28	-H28B	109.00	Cl31	-C30	-H30A	109.00
N26	-C28	-H28C	109.00	Cl31	-C30	-H30B	109.00
N26	-C28	-H28A	109.00	H30A	-C30	-H30B	108.00
H28A	-C28	-H28C	109.00	Cl31_a	-C30	-H30A	109.00
H28B	-C28	-H28C	109.00	Cl31_a	-C30	-H30B	109.00

See Table S5 for translation of symmetry code to equivalent positions.

Table S4. Torsion angles (°) for compound **1**·1/2CH_2Cl_2.

Se22	-Pt1	-Se21	-C23	9.8(3)
N7	-Pt1	-Se21	-C23	-169.6(4)
Se21	-Pt1	-Se22	-C27	-9.6(3)
N1	-Pt1	-Se22	-C27	173.2(4)
Se22	-Pt1	-N1	-C2	-1.6(9)
Se22	-Pt1	-N1	-C6	175.0(7)
N7	-Pt1	-N1	-C2	177.5(10)
N7	-Pt1	-N1	-C6	-5.9(7)
Se21	-Pt1	-N7	-C8	-172.4(7)
Se21	-Pt1	-N7	-C12	5.2(9)
N1	-Pt1	-N7	-C8	4.7(7)
N1	-Pt1	-N7	-C12	-177.7(9)
Pt1	-Se21	-C23	-S24	172.0(6)
Pt1	-Se21	-C23	-C27	-8.4(9)
Pt1	-Se22	-C27	-N26	-175.1(8)
Pt1	-Se22	-C27	-C23	7.9(10)
C30_a	-Cl31	-C30	-Cl31_a	0.0(15)
C30	-Cl31	-C30_a	-Cl31_a	0.0(13)
C25	-S24	-C23	-Se21	178.0(7)
C23	-S24	-C25	-N26	0.0(8)
C25	-S24	-C23	-C27	-1.7(9)
C23	-S24	-C25	-S27	179.1(8)
Pt1	-N1	-C6	-C5	-173.3(8)
Pt1	-N1	-C6	-C8	6.2(11)
C2	-N1	-C6	-C5	3.6(15)
C2	-N1	-C6	-C8	-176.9(10)
Pt1	-N1	-C2	-C3	173.3(8)
C6	-N1	-C2	-C3	-3.1(17)
Pt1	-N7	-C8	-C6	-2.8(11)
C12	-N7	-C8	-C9	0.7(15)
Pt1	-N7	-C12	-C11	-177.4(8)
C8	-N7	-C12	-C11	0.1(16)
Pt1	-N7	-C8	-C9	178.6(8)
C12	-N7	-C8	-C6	179.4(9)
C27	-N26	-C25	-S24	1.6(11)
C28	-N26	-C25	-S27	1.6(16)
C27	-N26	-C25	-S27	-177.5(9)
C28	-N26	-C25	-S24	-179.4(9)
C28	-N26	-C27	-Se22	0.7(14)
C28	-N26	-C27	-C23	177.9(10)
C25	-N26	-C27	-Se22	179.7(8)
C25	-N26	-C27	-C23	-3.0(13)
N1	-C2	-C3	-C4	1.9(18)
C2	-C3	-C4	-C5	-1.2(17)
C3	-C4	-C5	-C6	1.7(17)
C4	-C5	-C6	-C8	177.7(10)
C4	-C5	-C6	-N1	-2.8(16)
N1	-C6	-C8	-C9	176.3(10)
C5	-C6	-C8	-N7	177.2(10)
N1	-C6	-C8	-N7	-2.3(14)
C5	-C6	-C8	-C9	-4.2(17)
C6	-C8	-C9	-C10	179.9(10)
N7	-C8	-C9	-C10	-1.6(16)
C8	-C9	-C10	-C11	1.6(16)
C9	-C10	-C11	-C12	-0.9(16)
C10	-C11	-C12	-N7	0.0(17)
Se21	-C23	-C27	-Se22	0.4(14)
S24	-C23	-C27	-N26	2.9(12)
Se21	-C23	-C27	-N26	-176.8(7)
S24	-C23	-C27	-Se22	-179.9(6)

See Table S5 for translation of symmetry code to equivalent positions.

Table S5. Translation of symmetry code to equivalent positions for compound **1**·1/2CH_2Cl_2.

```
a =[  2666.00] = [  2_666] =1-x,1-y,1-z

b =[  2667.00] = [  2_667] =1-x,1-y,2-z

c =[  2567.00] = [  2_567] =-x,1-y,2-z

d =[  1565.00] = [  1_565] =x,1+y,z

e =[  2577.00] = [  2_577] =-x,2-y,2-z

f =[  2566.00] = [  2_566] =-x,1-y,1-z

g =[  2576.00] = [  2_576] =-x,2-y,1-z

h =[  2576.00] = [  2_576] =-x,2-y,1-z

j =[  1545.00] = [  1_545] =x,-1+y,z

k =[  2657.00] = [  2_657] =1-x,-y,2-z

l =[  1556.00] = [  1_556] =x,y,1+z

m =[  1554.00] = [  1_554] =x,y,-1+z

n =[  2666.00] = [  2_666] =1-x,1-y,1-z
```

Table S6. Half-wave potentials (V *vs* Fc^+/Fc) and electrochemical data recorded by CV on dmso solutions of complexes **1** and **2** (scan rate 50 mV s^{-1}).

		1	**2**
$E_{1/2}{}^{I}$	$E_{1/2}$	0.044	–0.027
	$\lvert E_{pc} - E_{pa} \rvert$	0.054	0.052
	i_{pc}/i_{pa}	0.5	0.9
$E_{1/2}{}^{II}$	$E_{1/2}$	–1.607	–1.620
	$\lvert E_{pc} - E_{pa} \rvert$	0.049	0.056
	i_{pc}/i_{pa}	1.2	1.1
$E_{1/2}{}^{III}$	$E_{1/2}$	–2.245	/
	$\lvert E_{pc} - E_{pa} \rvert$	0.048	/
	i_{pc}/i_{pa}	0.8	/

Table S7. Selected optimized bond lengths (Å) and angles (°) for complexes **1** and **2** in the gas phase and in CH_2Cl_2 (IEF-PCM SCRF model, in parenthesis).[a]

	1	**2**
Pt(13)-Se(22)	2.387 (2.401)	2.385 (2.398)
Pt(13)-Se(23)	2.385 (2.401)	2.382 (2.398)
Pt(13)-N(1)	2.059 (2.068)	2.066 (2.075)
Pt(13)-N(7)	2.058 (2.067)	2.064 (2.072)
Se(22)-C(27)	1.880 (1.87)	1.881 (1.888)
Se(21)-C(23)	1.871 (1.879)	1.872 (1.880)
C(27)-C(23)	1.359 (1.358)	1.359 (1.358)
Se(22)-Pt(13)-Se(21)	90.71 (90.97)	91.12 (91.38)
N(1)-Pt(13)-N(7)	79.20 (79.21)	79.97 (79.99)
N(1)-Pt-Se(21)-C(23)	0.00 (0.00)	0.00 (0.00)

[a] Atom labeling scheme as in Figure 1.

Table S8. Calculated eigenvalues *E* (eV) and composition (%) of frontier KS-MOs in terms of the central Pt atom and the N^N and Me-dset^{2-} ligands, and HOMO-LUMO energy gaps (eV) for complexes **1** and **2** in the gas phase and in CH_2Cl_2 (IEF-PCM SCRF model).

		$\Delta E_{HOMO-LUMO}$		*E*	N^N	Me-dset^{2-}	Pt
Gas	**1**	1.55	HOMO	–4.57	10	88	3
			LUMO	–3.02	85	9	6
	2	2.31	HOMO	–4.53	9	88	3
			LUMO	–2.97	86	9	6
CH_2Cl_2	**1**	1.56	HOMO	–5.00	4	91	5
			LUMO	–2.69	93	3	4
	2	2.34	HOMO	–4.99	4	91	5
			LUMO	–2.65	93	3	4

Table S9. NPA charges *Q* (e) calculated on Pt, Se(21), Se(22), N(1), N(7), the Me-dset^{2-} ligand and the diimmine N^N for **1** and **2** in the gas phase and in CH_2Cl_2 (IEF-PCM SCRF model).[a]

		1	**2**
Gas	*Q*(Pt13)	0.051	0.049
	Q(N1)	–0.452	–0.448
	Q(N7)	–0.454	–0.451
	Q(Se22)	0.074	0.074
	Q(Se21)	0.133	0.132
	Q(N^N)	0.305	0.314
	Q(Me-dset)	–0.357	–0.363
CH_2Cl_2	*Q*(Pt13)	0.061	0.059
	Q(N1)	–0.451	–0.447
	Q(N7)	–0.450	–0.448
	Q(Se22)	0.057	0.022
	Q(Se21)	0.019	0.060
	Q(N^N)	0.506	0.505
	Q(Me-dset)	–0.567	–0.564

[a] Atom labelling scheme as in Figure 1.

Table S10. Main electronic transitions (f > 0.010) calculated for **1** in CH_2Cl_2 (IEF-PCM SCRF model) at the TD-DFT level. For each transition, the excitation energy E (eV), the absorption wavelength λ (nm), the oscillator strength f, and the molecular orbital composition of the excite-state functions, along with the fragments where the involved KS-MOs are mainly localized, are reported.

Exc. state	E	λ	f	Composition[a]	%	Assignment
S1	1.751	708.0	0.135	117→118	99	Me-dset^{2-}(91%)→bipy(93%)
S5	2.849	435.2	0.012	117→120	97	Me-dset^{2-}(91%)→ bipy(98%)
S8	3.149	393.7	0.037	114→118	96	Me-dset^{2-}(82%)→ bipy(93%)
S11	3.691	335.9	0.227	117→122	83	Me-dset^{2-}(91%)→ Me-dset^{2-}(99%)
S12	3.790	327.1	0.067	113→121	62	Pt(93%)→ Me-dset^{2-}(42%)+Pt(39%)
				116→120	30	Me-dset^{2-}(75%)→ bipy(98%)
S13	3.800	326.3	0.012	116→120	61	Me-dset^{2-}(75%)→ bipy(98%)
				113→121	22	Pt(93%)→ Me-dset^{2-}(42%)+Pt(39%)
S17	4.146	299.0	0.017	114→119	95	Me-dset^{2-}(82%)→ bipy(98%)
S19	4.258	291.1	0.043	114→120	52	Me-dset^{2-}(82%)→ bipy(98%)
				112→118	39	bipy(85%)→ bipy(93%)
S23	4.357	284.5	0.062	109→118	32	Pt(42%)+ Me-dset^{2-}(31%)→ bipy(93%)
				114→120	22	Me-dset^{2-}(82%)→ bipy(98%)
				115→121	18	Me-dset^{2-}(99%)→ Me-dset^{2-}(42%)+Pt(39%)
S24	4.363	284.1	0.066	115→121	69	Me-dset^{2-}(99%)→ Me-dset^{2-}(42%)+Pt(39%)
S27	4.434	279.6	0.069	110→118	80	Pt(53%)+ Me-dset^{2-}(34%)→ bipy(93%)
S29	4.478	276.9	0.373	109→118	44	Pt(42%)+ Me-dset^{2-}(31%)→ bipy(93%)
				112→118	31	bipy(85%)→ bipy(93%)
S30	4.596	269.8	0.016	115→122	92	Me-dset^{2-}(99%)→ Me-dset^{2-}(99%)

[a] The MOs are labeled according to Figure 3.

Table S11. Static first hyperpolarizabilities β_{tot} (a.u. and esu) and static dipole moments μ (D) calculated for **1**and **2** in the gas phase and in CH_2Cl_2 (IEF-PCM SCRF model).

		1	**2**
Gas	$\beta_{tot}\cdot 10^4$ (a.u.)	4.26	4.81
	$\beta_{tot}\cdot 10^{-30}$ (esu)	368	416
	$\|\mu\|$ (D)	7.45	7.95
CH_2Cl_2	$\beta_{tot}\cdot 10^4$ (a.u.)	3.97	4.06
	$\beta_{tot}\cdot 10^{-30}$ (esu)	343	351
	$\|\mu\|$ (D)	11.08	11.66

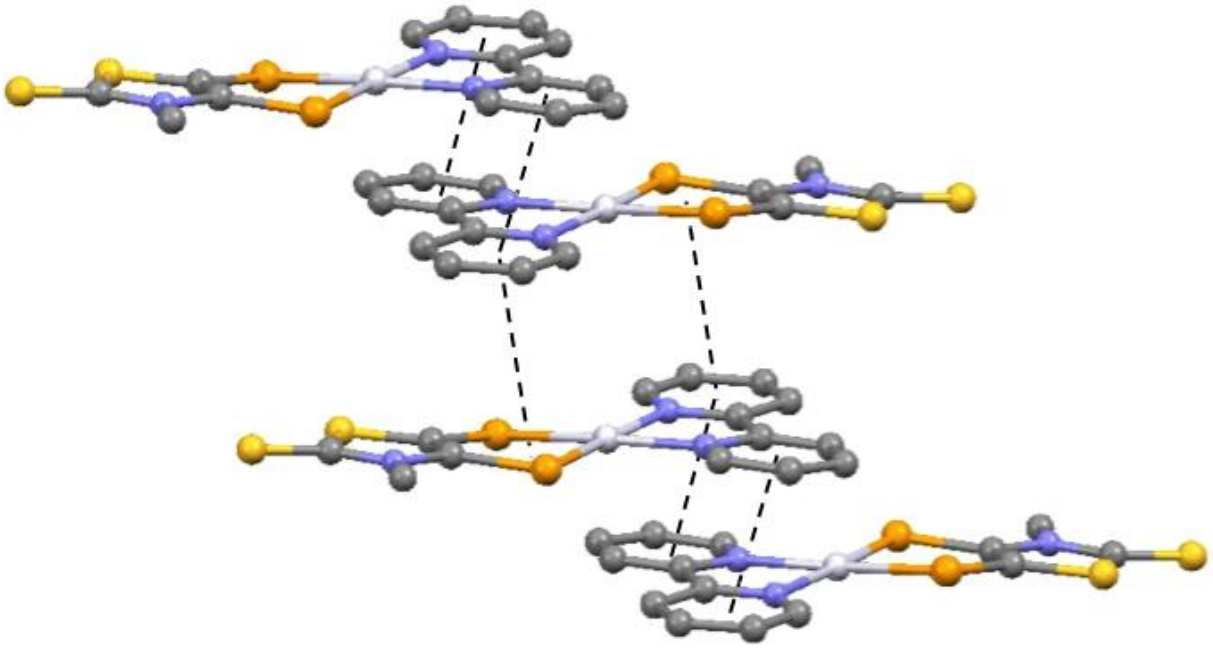

Figure S1. Drawing of a portion of the crystal packing of **1**·1/2CH_2Cl_2. Hydrogen atoms were omitted for clarity.

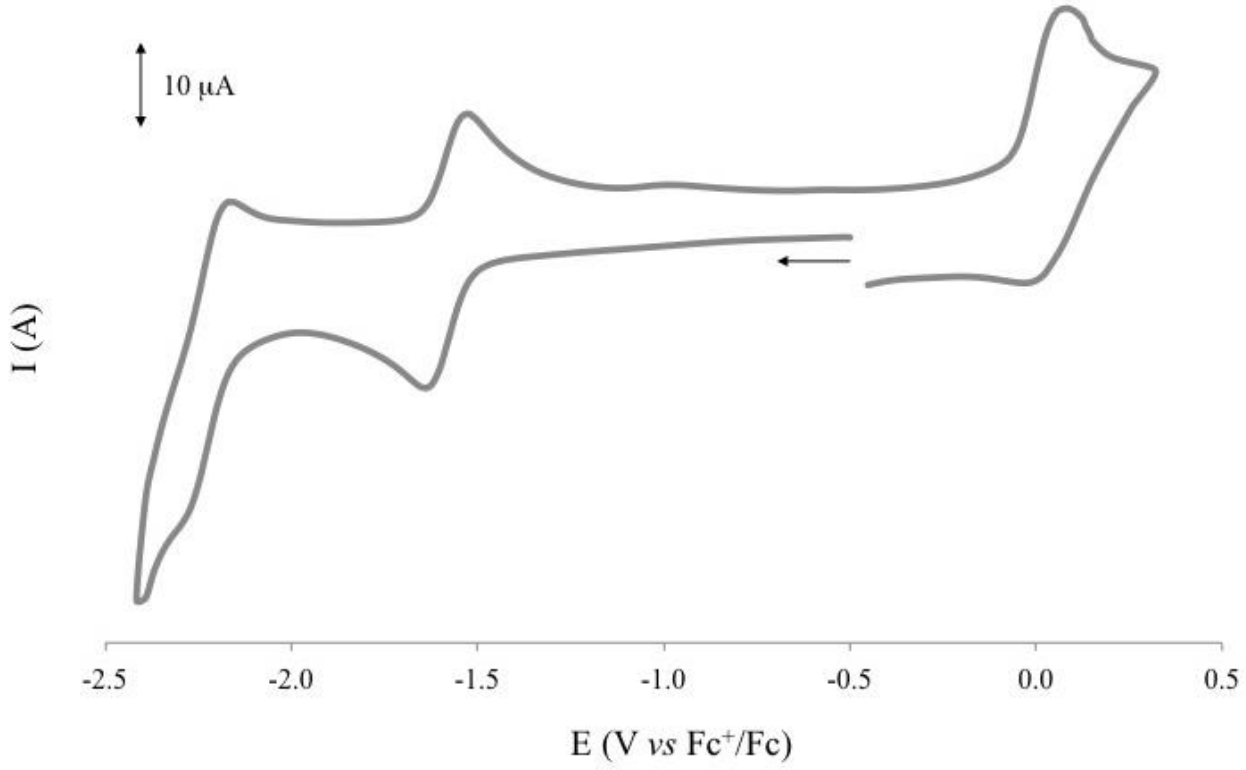

Figure S2. Cyclic voltammogram recorded at a platinum electrode on an anhydrous dmso solution of **1** [298 K; scan rate 50 mV s^{-1}; supporting electrolyte (TBA^+)(PF_6^-) 0.1 M].

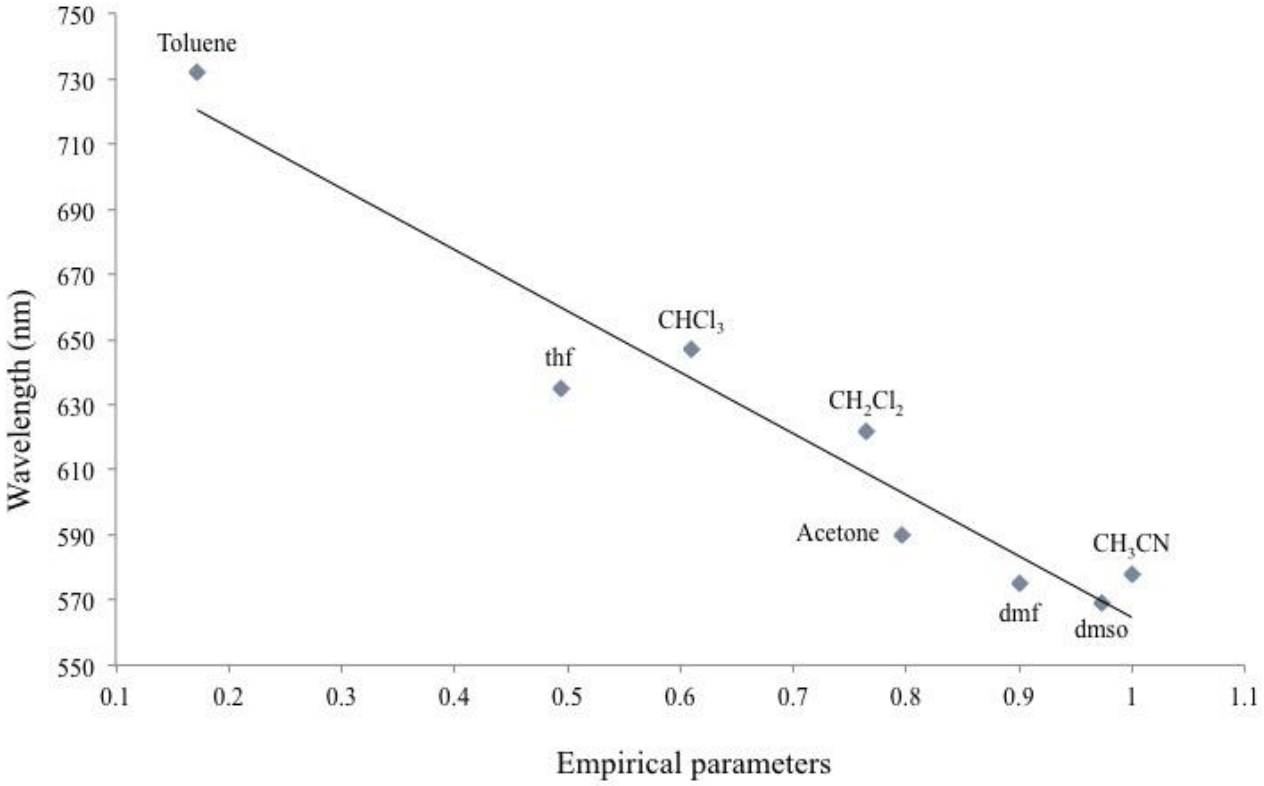

Figure S3. Correlation between the absorption maxima λ_{max} of the solvatochromic absorption in different solvents for complex **1** and the empirical scale formulated by Eisenberg for [Pt(N^N)(S^S)] complexes (R^2 = 0.93; Table 1; ref. 24).

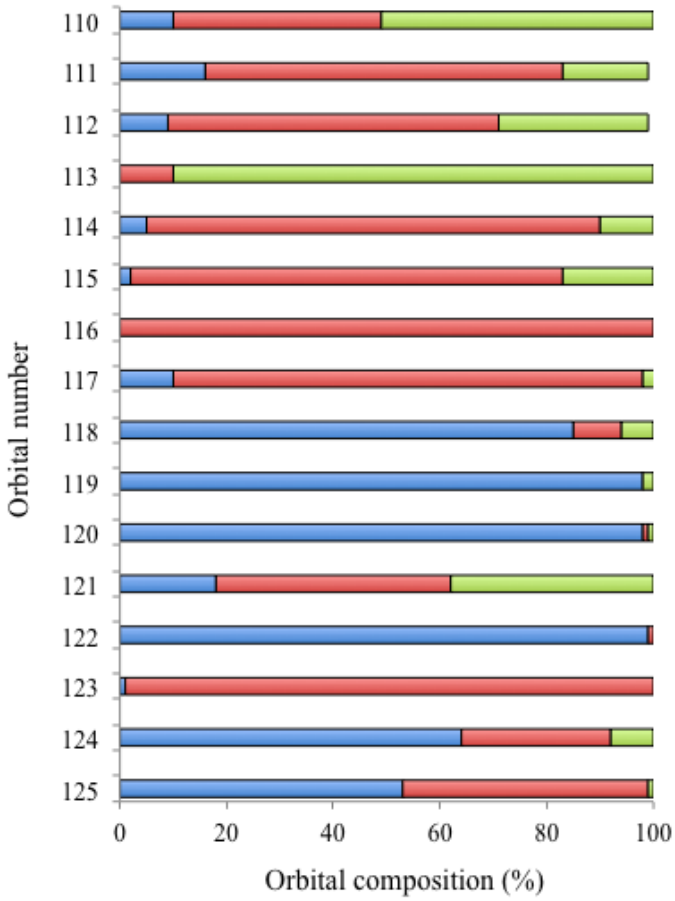

Figure S4. Frontier molecular orbital (KS-MOs 110-125; HOMO = 117, LUMO = 118) composition calculated for **1** in the gas phase [fragments: platinum atom (green); Me-dset^{2-} ligand (red); 2,2'-bipyridine (blue)].

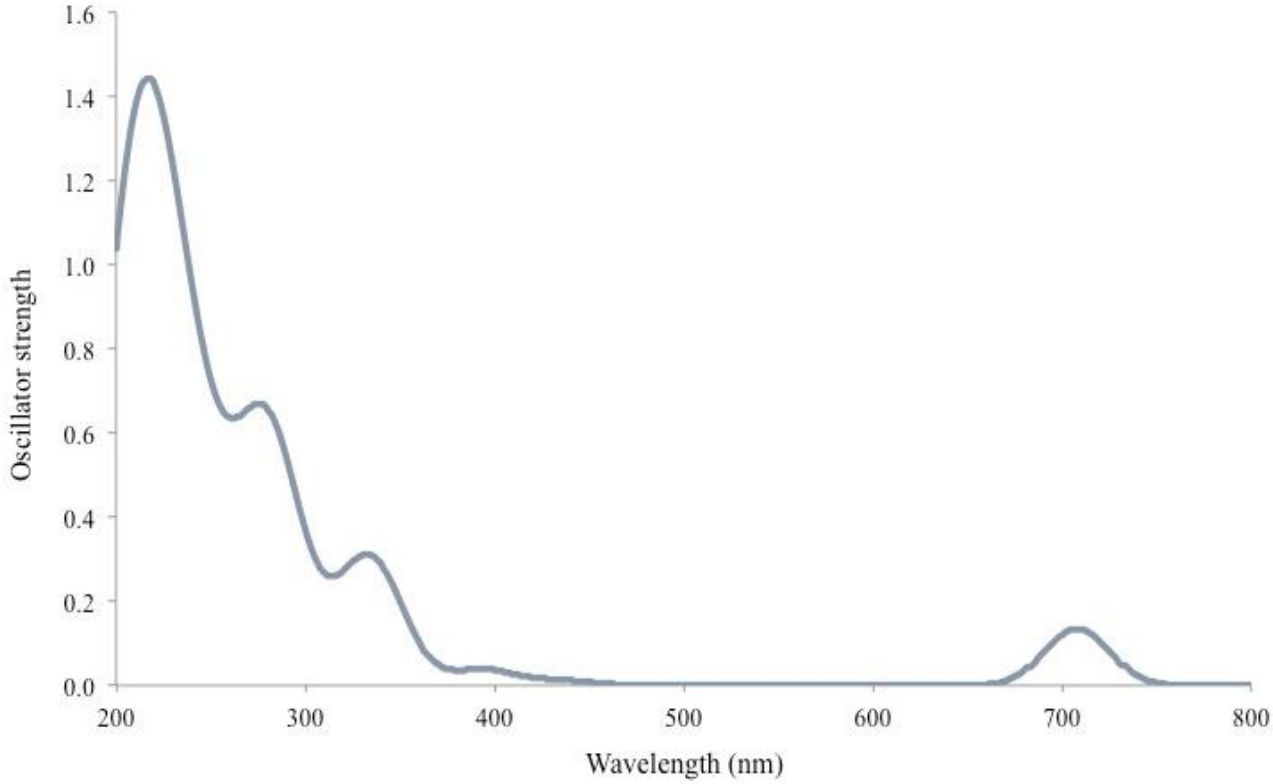

Figure S5. TD-DFT simulated UV-Vis absorption spectrum (200-800 nm) of complex **1** in CH_2Cl_2 (IEF-PCM SCRF model; Table S7).

References for Supporting Information

[1] G. T. Morgan, F. H. Burstall, *J. Chem. Soc.*, **1934**, 965-971.

[2] J. V. Rund, *Inorg. Chem.*, **1974**, *13*, 738-740.

[3] S. Eid, M. Formigué, T. Roisnel, D. Lorcy, *Inorg. Chem.*, **2007**, *46*, 10647–10654.

[4] A. Pintus, M. C. Aragoni, N. Bellec, F. A. Devillanova, D. Lorcy, F. Isaia, V. Lippolis, R. A. M. Randall, T. Roisnel, A. M. Z. Slawin, J. D. Woollins, M. Arca, *Eur. J. Inorg. Chem.*, **2012**, 3577–3594.

[5] http://www.unipress.waw.pl/fityk/.

[6] G. M. Sheldricks, *SHELXL-97*, University of Göttingen, Germany, **1997**.

[7] G. M. Sheldricks, *SHELXS-97*, University of Göttingen, Germany, **1997**.

Sheldrick, G. M. (2008). Acta Cryst. A64, 112–122.

[8] W. Koch, M. C. Holthausen, "A Chemist's Guide to Density Functional Theory", 2nd ed., Wiley-VCH, Weinheim, Germany, 2002.

[9] Gaussian 09, Revision A.02, M. J. Frisch, G. W. Trucks, H. B. Schlegel, G. E. Scuseria, M. A. Robb, J. R. Cheeseman, G. Scalmani, V. Barone, B. Mennucci, G. A. Petersson, H. Nakatsuji, M. Caricato, X. Li, H. P. Hratchian, A. F. Izmaylov, J. Bloino, G. Zheng, J. L. Sonnenberg, M. Hada, M. Ehara, K. Toyota, R. Fukuda, J. Hasegawa, M. Ishida, T. Nakajima, Y. Honda, O. Kitao, H. Nakai, T. Vreven, J. A. Montgomery Jr., J. E. Peralta, F. Ogliaro, M. Bearpark, J. J. Heyd, E. Brothers, K. N. Kudin, V. N. Staroverov, R. Kobayashi, J. Normand, K. Raghavachari, A. Rendell, J. C. Burant, S. S. Iyengar, J. Tomasi, M. Cossi, N. Rega, J. M. Millam, M. Klene, J. E. Knox, J. B. Cross, V. Bakken, C. Adamo, J. Jaramillo, R. Gomperts, R. E. Stratmann, O. Yazyev, A. J. Austin, R. Cammi, C. Pomelli, J. W. Ochterski, R. L. Martin, K. Morokuma, V. G. Zakrzewski, G. A. Voth, P. Salvador, J. J. Dannenberg, S. Dapprich, A. D. Daniels, O. Farkas, J. B. Foresman, J. V. Ortiz, J. Cioslowski, D. J. Fox, Gaussian, Inc., Wallingford CT, **2009**.

[10] C. Adamo, V. Barone, *J. Chem. Phys.*, **1999**, *110*, 6158-6170.

[11] A. Schäfer, H. Horn, R. Ahlrichs, *J. Chem. Phys.*, **1992**, *97*, 2571-2577.

[12] W. C. Ermler, R. B. Ross, P. A. Christiansen, *Int. J. Quant. Chem.*, **1991**, *40*, 829–846.

[13] T. H. Dunning Jr., P. J. Hay in "*Methods of Electronic Structure, Theory*", Vol. 2, H. F. Schaefer III ed., Plenum Press, **1977**.

[14] J. V. Ortiz, P. J. Hay, R. L. Martin, *J. Am. Chem. Soc.*, **1992**, *114*, 2736–2737.

[15] Average calculated Pt-Se bond length = 2.386 and 2.403 Å for the calculations performed with Ahlrichs pVDZ and CRENBL+ECP, respectively.

[16] A. E. Reed, R. B. Weinstock, F. Weinhold, *J. Chem. Phys.,* **1985**, *83,* 735–746.

[17] K. Wiberg, *Tetrahedron*, **1968**, *24*, 1083–1096.

[18] J. Tomasi, B. Mennucci, R. Cammi, *Chem. Rev.,* **2005**, *105*, 2999–3094.

[19] M. P. Cifuentes, M. G. Humphrey, *J. Organomet. Chem.*, 2004, 3968–3981.

[20] P. J. Mendes, A. J. P. Carvalho, J. P. P. Ramalho, *J. Mol. Struct.: THEOCHEM*, 2009, **900**, 110–117.

[21] Æ. Frisch, H. P. Hratchian, R. D. Dennington II, T. A. Keith, J. Millam, A. B. Nielsen, A. J. Holder, J. Hiscocks. Gaussian, Inc. GaussView Version 5.0, **2009**.

[22] G. Schaftenaar, J. H. Noordik, *J. Comput.-Aided Mol. Des.*, **2000**, *14*, 123–134.

[23] N. M. O'Boyle, A. L. Tenderholt, K. M. Langner, *J. Comput. Chem.*, **2008**, *29*, 839–845.

[24] S. D. Cummings, R. Eisenberg, *J. Am. Chem. Soc.*, **1996**, *118*, 1949–1960.